Journal of Biomechanics 82 (2019) 80–86

Contents lists available at ScienceDirect

Journal of Biomechanics

journal homepage: www.elsevier.com/locate/jbiomech
www.JBiomech.com

Quantitative assessment of 4D hemodynamics in cerebral aneurysms using proper orthogonal decomposition

Gábor Janiga

Lab. of Fluid Dynamics and Technical Flows, University of Magdeburg "Otto von Guericke", Universitätsplatz 2, Magdeburg D-39106, Germany

ARTICLE INFO

Article history:
Accepted 17 October 2018

Keywords:
Intracranial aneurysms
Computational fluid dynamics (CFD)
Phase-Contrast Magnetic Resonance Imaging (PC-MRI)
Proper orthogonal decomposition (POD)
Flow visualization
Quantitative comparison

ABSTRACT

Background and purpose: The comparison of different time-varying three-dimensional hemodynamic data (4D) is a formidable task. The purpose of this study is to investigate the potential of the proper orthogonal decomposition (POD) for a quantitative assessment.
Methods: The complex spatial-temporal flow information was analyzed using proper orthogonal decomposition to reduce the complexity of the system. PC-MRI blood flow measurements and computational fluid dynamic simulations of two subject-specific IAs were used to compare the different flow modalities. The concept of Modal Assurance Criterion (MAC) provided a further detailed objective characterization of the most energetic individual modes.
Results: The most energetic flow modes were qualitatively compared by visual inspection. The distribution of the kinetic energy on the modes was used to quantitatively compare pulsatile flow data, where the most energetic mode was associated to approximately 90% of the total kinetic energy. This distribution was incorporated in a single measure, termed spectral entropy, showing good agreement especially for Case 1.
Conclusion: The proposed quantitative POD-based technique could be a valuable tool to reduce the complexity of the time-dependent hemodynamic data and to facilitate an easy comparison of 4D flows, e.g., for validation purposes.

1. Introduction

Intracranial aneurysms are balloon-type dilatations of diseased brain arteries. It is hypothesized that hemodynamics play an essential role in the development of this disease, including the growth process (Meng et al., 2014) as well as the aneurysm rupture (Cebral et al., 2011).

The hemodynamic environment can, on the one hand, be studied experimentally: in vitro, e.g., using a Particle Image Velocimetry (PIV) technique, or in vivo such as Phase-Contrast Magnetic Resonance Imaging (PC-MRI). On the other hand, patient-specific computational fluid dynamics (CFD) is also a well-established tool to investigate the time-dependent three-dimensional (1D + 3D) blood flow conditions. The quantitative assessment of such time-dependent 4D flow representations is essential to understand the benefits or the limitations of a given approach.

Proper orthogonal decomposition (POD) is a relatively new method to analyze complex spatial-temporal information in intracranial flows. Byrne et al. (2014) first introduced this technique to quantify the flow instability in IAs. The eigenvalues of the system have been used to define the entropy of the system. Lower entropy values are attributed to stable flows. Higher values characterize unstable flows as quantified in a systematic study for an academic configuration by Abdelsamie et al. (2017) and further applied for biomedical flows in Daróczy et al. (2017), or even for transitional air flows during human exhalation (Voss et al., 2018).

Grinberg et al. (2009) used POD in stenosed carotid bifurcations to detect transitional flow in their CFD simulations. Kefayati and Poepping (2013) applied POD to study transitional flow in various stenosed silicone models using PIV experiments. Chang et al. (2017) studied the Wall Shear Stress conditions in a simplified Abdominal Aortic Aneurysm model using POD to build Reduced-Order Models. None of the above studies focused on the assessment of the dynamical behavior of different 4D flow representations; more specifically, none of them has applied POD for a detailed comparison of 4D flows, motivating the present study.

Simple comparison techniques based on probes are restricted to time-averaged values or to a given time instance, without capturing the dynamical behavior of the system. Time-varying analysis of

E-mail address: janiga@ovgu.de

https://doi.org/10.1016/j.jbiomech.2018.10.014
0021-9290/

flow forces or WSS is generally restricted to a single spatial probe location, e.g., capturing the maximum value over time. In the present study POD is suggested as a qualitative as well as a quantitative comparison method for assessing the dynamics of the entire time-dependent blood-flow in subject-specific cerebral aneurysms. Furthermore, POD can be efficiently used to identify and separate the smaller structures from the mean flow.

The application of proper orthogonal decomposition (POD) is still a pioneer in analyzing blood flows. In the present study, the potential of this method is further explored for the assessment of 4D hemodynamics. The successful application of this approach is illustrated for a two-dimensional bifurcation aneurysm and 4D blood flows in two subject-specific intracranial aneurysms obtained by 4D PC-MRI measurements and CFD simulations. It was not aimed to validate the presented flows, but rather to propose a quantitative assessment for the comparison of arbitrary 4D flow data.

2. Material and methods

2.1. Demonstration case: two-dimensional bifurcation aneurysm

In order to carry out POD-based flow comparisons, first, a simple two-dimensional bifurcation aneurysm geometry was investigated. Unsteady finite-volume computations were performed in two widely known commercial CFD-solvers – ANSYS Fluent 17.0 (Ansys Inc., Canonsburg, PA, USA) and StarCCM+11.02 (Siemens Product Lifecycle Management Software Inc., Plano, TX, USA) – using the same settings and assumptions as summarized next. Pulsatile flow rate was prescribed at the inlet of the domain and no-slip condition was applied on the walls. Constant relative pressure was assumed at the outlets. The high-quality block-structured quadrilateral mesh was created in ANSYS ICEM-CFD (Ansys Inc., Canonsburg, PA, USA). The second-order temporal discretization was applied for 10 000 equal-size time steps in a cardiac cycle with 30 inner iterations. A Newtonian fluid was assumed with a density of 1045 kg/m^3 and a dynamic viscosity of 0.004 $Pa \cdot s$. The gradient information on the finite-volume cell boundaries was treated by the Green-Gauss method during the segregated solution of the governing equations assuming laminar flow. Every 50th time steps from the simulated second heart-cycle, corresponding to a total of 200 snapshots, were considered in the POD analysis, where only the sac of the aneurysm was investigated.

2.2. Case details

The suggested methods based on proper orthogonal decomposition are illustrated for an anterior communicating artery (AcomA) aneurysm of a 59-year-old female patient (Case 1) and for a left middle cerebral artery (MCA) aneurysm of a 51-year-old male patient (Case 2). The PC-MRI flow measurements conducted on a 7Tesla (Siemens Magnetom) whole-body MRI system and CFD computations using subject-specific inflow condition were examined here. For the sake of brevity, the reader is referred to Berg et al. (2014) for further details regarding the PC-MRI data acquisition, and for the time-dependent CFD simulation.

2.3. POD analysis

Using the POD method, the 4D flow information is decomposed as a series of distinct spatial modes $\varphi(r)$ (independent from time) and time coefficients $a(t)$ (independent from the spatial information):

$$u(r,t) = \sum_{k=1}^{N} a^k(t) \cdot \varphi^k(r). \tag{1}$$

The computed modes are orthogonal and vector variables, similar to the velocity vectors. With their linear combination, the original flow field can be reconstructed as an ensemble of a given number of N snapshots. The POD computations require the solution of an eigenvalue system, as explained elsewhere, e.g., in Byrne (2013) and Abdelsamie et al. (2017). The sum of the eigenvalues gives the total kinetic energy of the considered flow. The resulting eigenvalues can be sorted, defining the dominance of the kinetic energy associated with a given mode. The POD method can be efficiently used to characterize specific flow features, so-called coherent structures. Thus, the main primary flow can be easily separated from the underlying secondary or tertiary flow structures. The first mode – the most energetic, having the largest eigenvalue – represents the time-averaged flow field. The second and third modes – accompanied by the second and third largest eigenvalues – characterize the secondary and tertiary flows, respectively.

The POD analysis is demonstrated for both the PC-MRI as well as for CFD results. The total number of available time steps obtained by the PC-MRI measurements – nine time steps for Case 1 and fourteen time steps for Case 2 – were considered in a cardiac cycle, incorporating the three-dimensional flow velocities. These velocities are defined in their own separate coordinate systems, i.e., a Cartesian equidistant voxel-grid for the PC-MRI data with a resolution of $0.75 \times 0.75 \times 0.8$ mm and an unstructured tetrahedral mesh – less than 0.3 mm resolution – with prism layers for the CFD results. An advantage of the present method is that no data interpolation is required to a common system, i.e., a common mesh, therefore, even different mesh resolutions – or even mesh types – can be applied as illustrated in the present study.

The eigenvalues of the POD analysis can be further used, e.g., for data reduction. The cumulative value of the eigenvalues – i.e., the sum of the first few eigenvalues – can be used to determine how many modes are required to represent, e.g., 90%, 95%, or 99% kinetic energy of a given system. Usually much fewer modes than the available number of snapshots are sufficient for a quite accurate description. It allows the construction of a reduced-order model. In this study, all the modes are considered to represent the total amount of the kinetic energy.

2.4. Modal Assurance Criterion (MAC)

Assuming the same grid representation, further detailed quantitative assessment can be performed. A convenient concept, the Modal Assurance Criterion (MAC), can be applied to quantitatively summarize the correlations between all possible POD modes (Allemang, 2003). It is expressed as

$$\mathrm{MAC}_{i,j} = \frac{\left|\Phi_i^T \Psi_j\right|^2}{\left(\Phi_i^T \Phi_i\right) \cdot \left(\Psi_j^T \Psi_j\right)}, \tag{2}$$

where Φ denotes the i^{th} POD mode obtained from the measured velocity and Ψ is the j^{th} computed POD mode from the computed velocity after interpolation. The elements of the MAC matrix can be presented in table formats, but 2D or 3D graphical representations are also possible. The MAC matrix defines the degree of linearity between two fields, in the present case between the scalar valued magnitudes of the POD vector modes. Normalization of the modes is not required before calculating the elements of the MAC matrix. A perfect match would yield a correlation factor of one; otherwise, a low correlation factor, approaching zero, corresponds to poor agreement. The MAC matrix is usually used in mechanics, e.g., comparing vibration modes, but it can also be well used for comparing experimental and simulated flow data (Andrianne et al., 2012).

In the present application, the mesh resolution was different, therefore, an interpolation was necessary: the computed values of the finer CFD mesh were interpolated to the coarser grid defined by the PC-MRI resolution, enabling a direct comparison of the different modes on the common grid locations.

As pointed out by Allemang (2003) the missing interpolated values should be removed before calculating the elements of the MAC matrix. Otherwise, they can negatively affect the obtained correlations.

2.5. Root-mean-square error of the POD modes

The root-mean-square (RMS) error is introduced as an estimator to determine the number of required modes. This metric for the velocity can be defined as:

$$rms^M = \sqrt{\frac{1}{N_{cell}} \sum_{i=1}^{N_{cell}} \left[\left(u^M_{reco} - u_{sim}\right)^2 + \left(v^M_{reco} - v_{sim}\right)^2 + \left(w^M_{reco} - w_{sim}\right)^2 \right]}, \tag{3}$$

where N_{cell} denotes the number of mesh cells involved in the analysis, u^M_{reco}, v^M_{reco} and w^M_{reco} correspond to the reconstructed velocity components using the first M modes. The original velocity components u_{sim}, v_{sim} and w_{sim} are obtained from the numerical simulation. They can be reconstructed with help of the POD modes. The reconstruction can be improved by increasing the number of considered modes, M.

3. Results

3.1. POD-based comparison for the two-dimensional bifurcation aneurysm

Fig. 1 illustrates the first 6 POD vector modes for the 2D bifurcation aneurysm case obtained from the unsteady velocity vector field. No differences can be visually observed comparing the velocity fields of the two computations using the same setups in the two different solvers. As a result, the investigated POD modes obtained from these tools cannot be distinguished qualitatively in the aneurysm sac.

The MAC matrix representation in Fig. 2(a) makes a quantitative comparison possible. The perfect match between these modes can be appreciated, as the elements in the main diagonal are typically ones. The calculation of the elements in the MAC matrix involve all

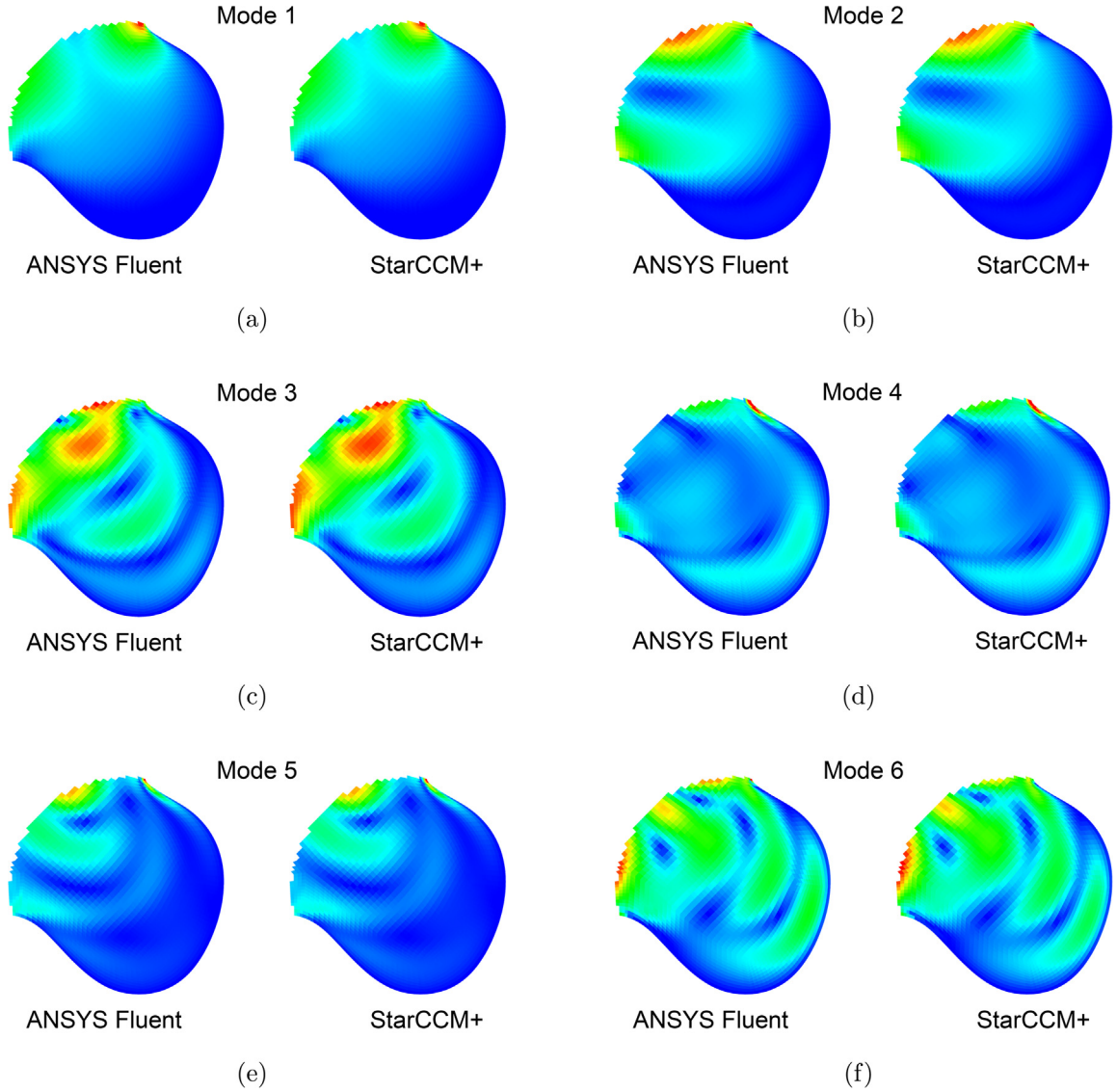

Fig. 1. Comparison of the first six energetic POD modes for the 2D bifurcation aneurysm case obtained by ANSYS Fluent and StarCCM+.

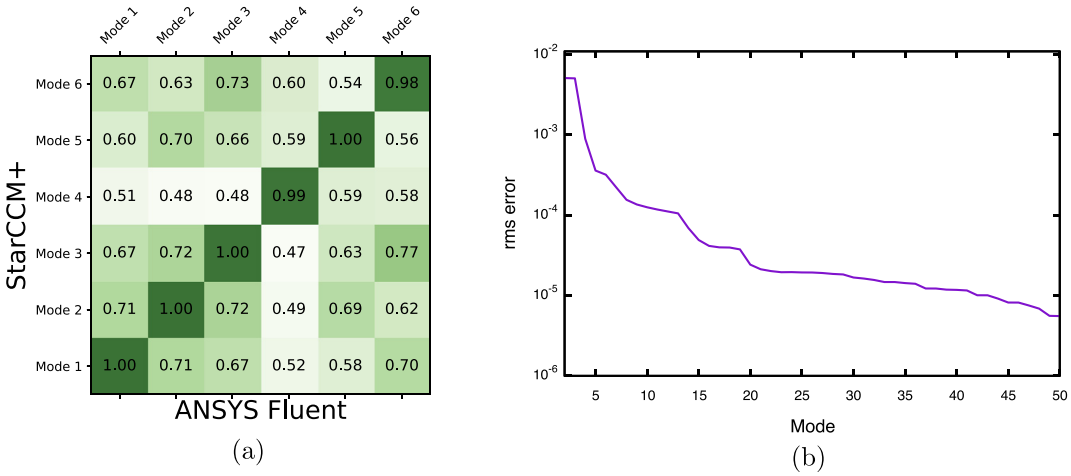

Fig. 2. Left: MAC criterion for the 2D bifurcation aneurysm case comparing the POD modes obtained by ANSYS Fluent and StarCCM+. An excellent match can be observed in the main diagonal. Higher values are highlighted by darker colors. Right: the RMS error of the reconstructed velocity field as a function of the number of applied modes in the reconstruction.

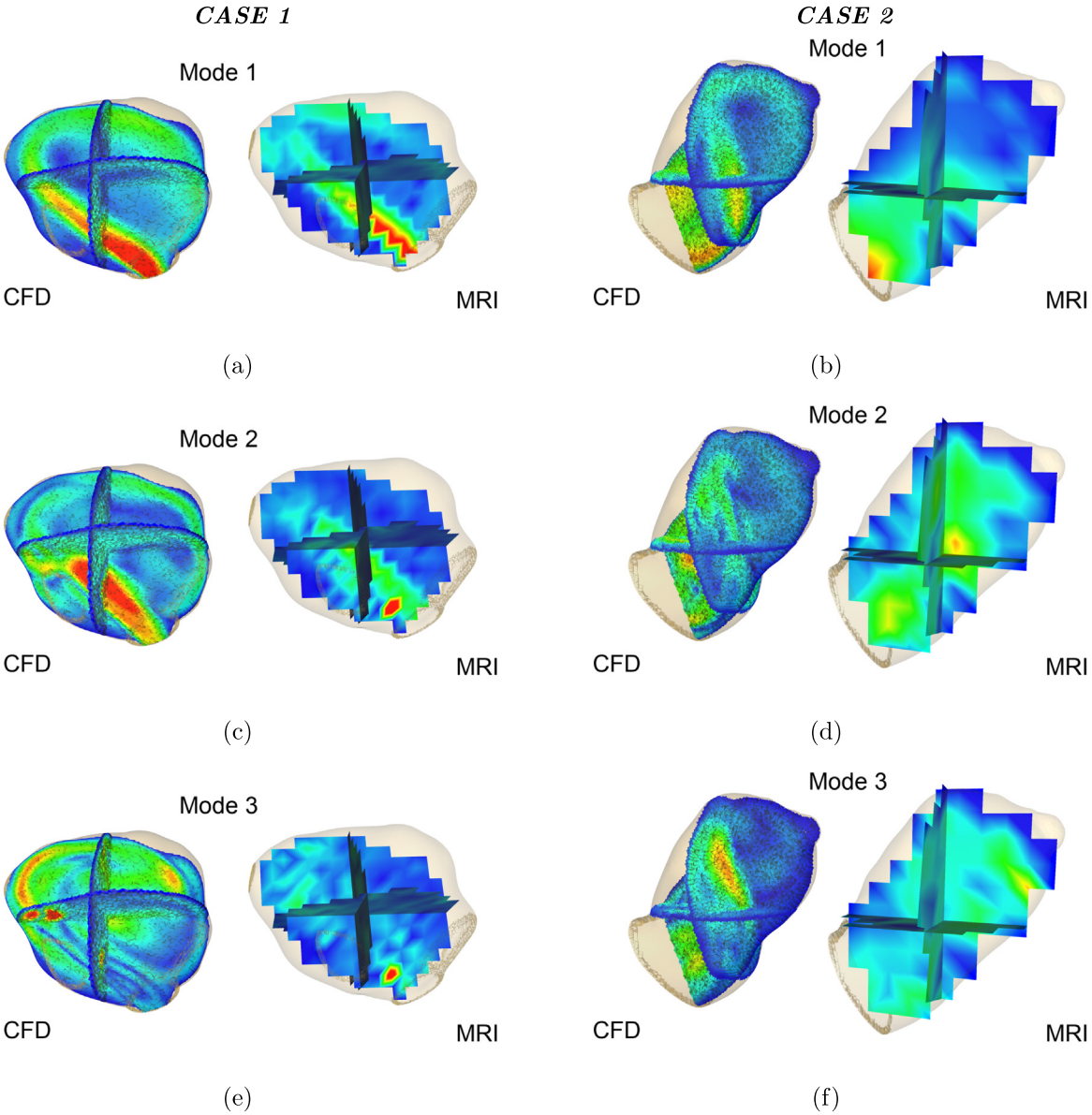

Fig. 3. Comparison of the most energetic three CFD and PC-MRI POD mode magnitude fields in selected cutplanes: Case 1 left, Case 2 right.

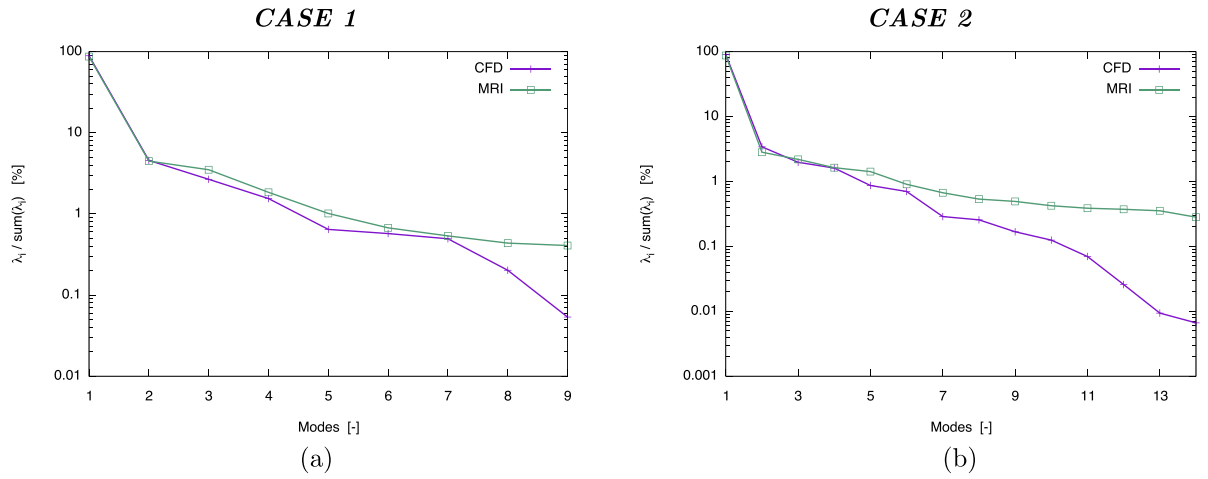

Fig. 4. Normalized eigenvalues λ_i of the considered POD analyses for PC-MRI measurements and for the CFD simulations, representing the distribution of the relative kinetic energy on the modes: Case 1 left, Case 2 right.

the finite volume cells in the region of interest; therefore, partial match can also be evaluated providing values tending toward zero.

The RMS error (Eq. (3)) of the reconstructed velocity field for the 2D aneurysm case is illustrated in Fig. 2(b) as a function of the number of applied modes in the reconstruction. This figure illustrates, that a fairly good reconstruction is achieved using only four modes, yielding an RMS error less than 10^{-3}. However, a very good reconstruction is possible with 15 modes, where the RMS error drops below 10^{-4}.

3.2. Comparison of PC-MRI and CFD

The three most energetic modes for the measured PC-MRI data and for the simulated CFD results showing the vector magnitudes of the modes in selected cutplanes are illustrated in Fig. 3. A good qualitative agreement can be observed for the first modes and a fair agreement for the second and third modes. This underlines the previous observations shown by Berg et al. (2014), which showed a good, but not a perfect match.

The obtained POD modes are vector variables. Ordering the corresponding eigenvalues of the POD computations, their dominance can be determined by considering the kinetic energy of the system. They can be used for further analysis, in a quantitative manner, by comparing the eigenvalues of the POD system. The kinetic energy distribution of the computed POD modes is depicted in Fig. 4 and quantitatively summarized in Table 1. This distribution of the kinetic energy can be incorporated in a single measure, termed spectral entropy (Byrne, 2013; Abdelsamie et al., 2017). A very good agreement can be observed for Case 1 as shown in Table 1: 0.57 for PC-MRI measurement and 0.60 for the CFD simulation.

For Case 1, the first eigenvalues for the experimental and simulated cases are 87.4% and 88.2%, respectively. This surprisingly good agreement indicates that the first mode – corresponding to the temporal mean velocity – represents almost 90% of the total kinetic energy for both cases. The agreement for the second eigenvalues is also good: 4.4% for the PC-MRI measurements and 5.3% for the CFD computations. They represent the dominance of the secondary flow structures. The third eigenvalues – although their importance is rather low in these cases – also agree well, with 3.5% and 2.8% for the PC-MRI data and for the CFD results, respectively.

For Case 2, the first eigenvalues are 87.5% and 90.5% for the experimental and simulated cases, respectively. The second eigenvalues show good agreement, with 2.8% for the PC-MRI measurements and 3.4% for the CFD computations. The third eigenvalues agree exceptionally well: 2.2% and 2.0% for the experimental and simulated cases, respectively.

Table 1
Eigenvalues of the considered POD analyses for PC-MRI and CFD.

Eigenvalues	AcomA (Case 1)		MCA (Case 2)	
	MRI	CFD	MRI	CFD
1	87.4%	88.2%	87.5%	90.5%
2	4.4%	5.3%	2.8%	3.4%
3	3.5%	2.8%	2.2%	2.0%
4	1.8%	1.5%	1.6%	1.6%
5	1.0%	0.7%	1.4%	0.9%
6	0.6%	0.6%	0.9%	0.7%
7	0.5%	0.6%	0.7%	0.3%
8	0.4%	0.2%	0.5%	0.3%
Spectral entropy	0.57	0.60	0.49	0.66

This quantitative comparison of the eigenvalues illustrates that the dominance of these POD flow modes are almost identical for both investigated flow representations.

In order to apply the MAC criterion, an interpolation of the different results is required if they are not already defined on the same locations. In this study, the modes obtained on the finer CFD mesh were interpolated on the coarser PC-MRI grid. The first four energetic modes were involved in the MAC criterion as displayed in Fig. 5. It is apparent, that the main diagonal represents the comparison of the same corresponding mode numbers. A reasonably good match can be observed in Fig. 5, despite the limited temporal and spatial resolution of the PC-MRI experiments. Unfortunately, the small number of voxels within the small MCA aneurysm (Case 2) makes this comparison very sensitive.

4. Discussion

CFD simulations are often validated with different in vivo or in vitro flow measurements. In-vivo and in vitro measurements more often produce time-varying flow information, but CFD simulations are also commonly performed to reproduce the time-dependent hemodynamic environment. It is crucial to evaluate quantitatively the different flow representations in order to understand the differences and their limitations.

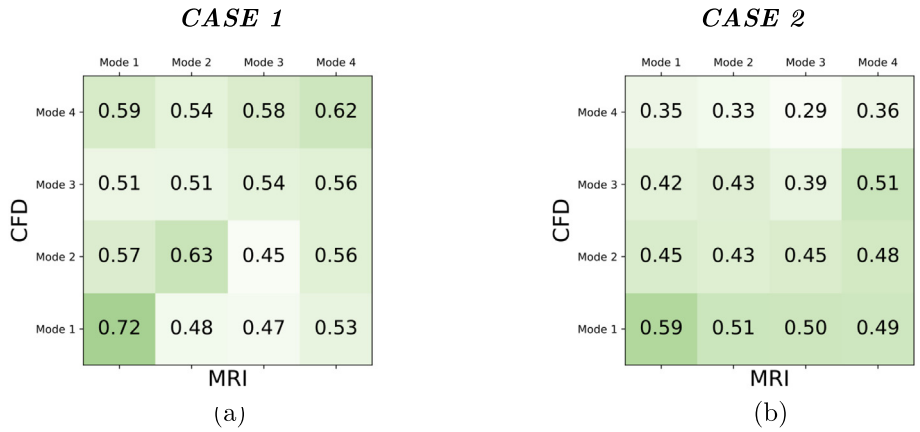

Fig. 5. MAC criterion for Case 1 (left) and Case 2 (right). A good match corresponds to a factor of close to one and a low correlation factor approaching zero, corresponds to poor agreement. Higher values are highlighted by darker colors.

The complexity of the time-dependent flow data can be partially eliminated by computing the temporal average, or only considering a specific time step such as the peak systolic.

Raschi et al. (2012) evaluated computed flow velocity with PIV experiments using the angular similarity index (ASI) and the magnitude similarity index (MSI). Berg et al. (2014) compared 4D blood flow information obtained from PC-MRI and CFD computations. The velocity vectors are analyzed in random point probe locations in given time instances, comparing their magnitudes (MSI) and the angles (ASI) between them. Velocity distributions and profiles are qualitatively shown in given cut-planes. Paliwal et al. (2017) validated CFD computations with PIV measurements in silicone phantom models considering the various uncertainties of these methods.

Recently, DSA-based flow reconstruction techniques were compared with 2D-projected hemodynamic simulations averaging the flow in time (Cebral et al., 2017), but 4D DSA can directly deliver time-resolved 3D imaging of cerebral vessels (Lang et al., 2017).

On the other hand, various CFD simulations are often evaluated as well. Different hemodynamic computations can also be compared with one another, e.g., to assess the effects of generalized or subject-specific boundary conditions, but different numerical results can also be compared, as performed in various CFD challenges (Steinman et al., 2013; Berg et al., 2015). The temporal dynamics of the flow data is often neglected in the evaluation of the 4D hemodynamic data, despite the wide range of possible applications.

The POD analyses include both the spatial as well as the temporal information. In the POD analysis suggested here, the complex temporal-spatial information is decomposed into spatial and temporal parts without losing the time evolution. It is therefore well-suited for the investigation of time-varying data and for reducing the complexity of the system.

Although various other possible linear decomposition approaches are also possible, as pointed out by Holmes et al. (1996), the POD method yields an optimal basis for a given number of modes. The obtained kinetic energy, on average, is maximized on the subspace defined by these leading modes.

The eigenvalues obtained by the POD analysis provide the distribution of the kinetic energy on the obtained modes. The direct inspection of these eigenvalues facilitates an easy quantitative comparison of different flow representations. The advantage of this method is that no co-registration or no mesh interpolation is required; therefore, it can be used for different grids, as well as for different temporal resolutions.

A further benefit is that the method is quite insensitive to the number of available snapshots, as illustrated, e.g., for isotropic turbulence (Abdelsamie et al., 2017). As reported by Kefayati and Poepping (2013) in a POD-analysis for PIV-measurements in arterial bifurcations, the selection of a different number of snapshots has shown only a negligible effect on the eigenvalues. In the present study, if twice as many snapshots were involved in the POD analysis of the CFD results, no noticeable change could be found for the first five most energetic modes, proving the robustness of this approach.

It should be kept in mind that the POD analysis was restricted here to merely the region of interest, i.e., for the aneurysm lumen separated from artery. The first eigenvalue corresponding to the first mode represented around 90% of the total energy in the presented cases, however, including the entire computational domain together with the inlet and outlet sections would have yielded more than 97%. This signifies that, considering the entire computational domain, the energy contribution of the mean flow represented by the first mode would be much stronger and would leave only a small amount of remaining kinetic energy on the higher modes.

The following limitations should be taken into consideration for the interpretation of the presented results. The determination of the MAC matrix is quite sensitive in respect of the location of the geometries, therefore, a careful co-registration of the different domains is required. Furthermore, an interpolation of the results should be performed and the values should be defined on the same probe locations. This interpolation might produce further uncertainties. Despite many improvements regarding MRI resolution in recent years, measurements of cerebral arteries are still challenging and the resolution remains limited, especially for small aneurysms, where the co-registration with CFD data is difficult. Nevertheless, the suggested POD method can be used for assessing 4D flows, even if a perfect match could not be achieved yet.

5. Conclusions

Qualitative and quantitative methods were introduced for the comparison of various time-dependent blood flow data. The suggested POD analysis allowed a robust and a global assessment, which is less sensitive to local disturbances. The complexity of the time-dependent hemodynamic data can successfully be reduced by applying this method. The computed POD eigenvalues do not require the same grid resolution for the different flow representations. Therefore, it can easily be applied for different meshes, but also for a different number of snapshots. The normalized kinetic energy provides a useful metric to quantitatively

compare the dominant flow structures. The application of the MAC criterion – assuming the same mesh – for the decomposed flow modes can provide a further quantitative approach for an objective evaluation. Therefore, the proposed method could be a valuable tool to objectively examine different hemodynamic simulations and it could also be used to validate computations with in vivo or in vitro time-varying flow measurements.

Conflict of interest

None.

Acknowledgment

This work was partly funded by the Federal Ministry of Education and Research in Germany within the Research Campus STIMULATE under Grant No. 13GW0095A.

References

Abdelsamie, A., Janiga, G., Thévenin, D., 2017. Spectral entropy as a flow state indicator. Int. J. Heat Fluid Flow 68, 102–113. https://doi.org/10.1016/j.ijheatfluidflow.2017.09.013.

Allemang, R.J., 2003. The modal assurance criterion – twenty years of use and abuse. Sound Vib. 2003, 14–21 <http://www.sandv.com/downloads/0308alle.pdf>.

Andrianne, T., Guissart, A., Terrapon, V., Dimitriadis, G., 2012. Using proper orthogonal decomposition methods for comparing CFD results to experimental measurements. In: Proceedings of the 5th Symposium on Integrating CFD and Experiments in Aerodynamics (Integration 2012), pp. 55–66.

Berg, P., Roloff, C., Beuing, O., Voss, S., Sugiyama, S.I., Aristokleous, N., Anayiotos, A. S., Ashton, N., Revell, A., Bressloff, N.W., Brown, A.G., Chung, B.J., Cebral, J.R., Copelli, G., Fu, W., Qiao, A., Geers, A.J., Hodis, S., Dragomir-Daescu, D., Nordahl, E., Suzen, Y.B., Khan, M.O., Valen-Sendstad, K., Kono, K., Menon, P.G., Albal, P.G., Mierka, O., Münster, R., Morales, H.G., Bonnefous, O., Osman, J., Goubergrits, L., Pallares, J., Cito, S., Passalacqua, A., Piskin, S., Pekkan, K., Ramalho, S., Marques, N., Sanchi, S., Schumacher, K.R., Sturgeon, J., Švihlová, H., Hron, J., Usera, G., Mendina, M., Xiang, J., Meng, H., Steinman, D.A., Janiga, G., 2015. The computational fluid dynamics rupture challenge 2013 – Phase II: variability of hemodynamic simulations in two intracranial aneurysms. J. Biomech. Eng. 137, 121008. https://doi.org/10.1115/1.4031794.

Berg, P., Stucht, D., Janiga, G., Beuing, O., Speck, O., Thévenin, D., 2014. Cerebral blood flow in a healthy circle of Willis and two intracranial aneurysms: computational fluid dynamics versus four-dimensional phase-contrast magnetic resonance imaging. J. Biomech. Eng. 136, 041003. https://doi.org/10.1115/1.4026108.

Byrne, G., Mut, F., Cebral, J., 2014. Quantifying the large-scale hemodynamics of intracranial aneurysms. Am. J. Neuroradiol. 35, 333–338. https://doi.org/10.3174/ajnr.A3678.

Byrne, G.A., 2013. Cortex-based spatiotemporal characterization of nonlinear flows (Ph.D. thesis). George Mason University.

Cebral, J., Mut, F., Chung, B.J., Spelle, L., Moret, J., Van Nijnatten, F., Ruijters, D., 2017. Understanding angiography-based aneurysm flow fields through comparison with computational fluid dynamics. Am. J. Neuroradiol. 38, 1180–1186. https://doi.org/10.3174/ajnr.A5158.

Cebral, J.R., Mut, F., Weir, J., Putman, C., 2011. Quantitative characterization of the hemodynamic environment in ruptured and unruptured brain aneurysms. Am. J. Neuroradiol. 32, 145–151. https://doi.org/10.3174/ajnr.A2419.

Chang, G.H., Schirmer, C.M., Modarres-Sadeghi, Y., 2017. A reduced-order model for wall shear stress in abdominal aortic aneurysms by proper orthogonal decomposition. J. Biomech. 54, 33–43. https://doi.org/10.1016/j.jbiomech.2017.01.035.

Daróczy, L., Abdelsamie, A., Janiga, G., Thévenin, D., 2017. State detection and hybrid simulation of biomedical flows. In: 10th International Symposium on Turbulence and Shear Flow Phenomena, Chicago-IL, USA, pp. 280/1–6.

Grinberg, L., Yakhot, A., Karniadakis, G.E., 2009. Analyzing transient turbulence in a stenosed carotid artery by proper orthogonal decomposition. Ann. Biomed. Eng. 37, 2200–2217. https://doi.org/10.1007/s10439-009-9769-z.

Holmes, P.J., Lumley, J.L., Berkooz, G., 1996. Turbulence, coherent structures, dynamical systems and symmetry. Cambridge.

Kefayati, S., Poepping, T.L., 2013. Transitional flow analysis in the carotid artery bifurcation by proper orthogonal decomposition and particle image velocimetry. Med. Eng. Phys. 35, 898–909. https://doi.org/10.1016/j.medengphy.2012.08.020.

Lang, S., Gölitz, P., Struffert, T., Rösch, J., Rössler, K., Kowarschik, M., Strother, C., Doerfler, A., 2017. 4D DSA for dynamic visualization of cerebral vasculature: a single-center experience in 26 cases. Am. J. Neuroradiol. 38, 1169–1176. https://doi.org/10.3174/ajnr.A5161.

Meng, H., Tutino, V.M., Xiang, J., Siddiqui, A., 2014. High WSS or low WSS? Complex interactions of hemodynamics with intracranial aneurysm initiation, growth, and rupture: toward a unifying hypothesis. Am. J. Neuroradiol. 35, 1254–1262. https://doi.org/10.3174/ajnr.A3558.

Paliwal, N., Damiano, R.J., Varble, N.A., Tutino, V.M., Dou, Z., Siddiqui, A.H., Meng, H., 2017. Methodology for computational fluid dynamic validation for medical use: application to intracranial aneurysm. J. Biomech. Eng. 139, 121004. https://doi.org/10.1115/1.4037792.

Raschi, M., Mut, F., Byrne, G., Putman, C.M., Tateshima, S., Viñuela, F., Tanoue, T., Tanishita, K., Cebral, J.R., 2012. CFD and PIV analysis of hemodynamics in a growing intracranial aneurysm. Int. J. Numer. Methods Biomed. Eng. 28, 214–228. https://doi.org/10.1002/cnm.1459.

Steinman, D.A., Hoi, Y., Fahy, P., Morris, L., Walsh, M.T., Aristokleous, N., Anayiotos, A.S., Papaharilaou, Y., Arzani, A., Shadden, S.C., Berg, P., Janiga, G., Bols, J., Segers, P., Bressloff, N.W., Cibis, M., Gijsen, F.H., Cito, S., Pallarés, J., Browne, L.D., Costelloe, J.A., Lynch, A.G., Degroote, J., Vierendeels, J., Fu, W., Qiao, A., Hodis, S., Kallmes, D.F., Kalsi, H., Long, Q., Kheyfets, V.O., Finol, E.A., Kono, K., Malek, A.M., Lauric, A., Menon, P.G., Pekkan, K., Moghadam, E., Marsden, A.L., Oshima, M., Katagiri, K., Peiffer, V., Mohamied, Y., Sherwin, S.J., Schaller, J., Goubergrits, L., Usera, G., Mendina, M., Valen-Sendstad, K., Habets, D.F., Xiang, J., Meng, H., Yu, Y., Karniadakis, G.E., Shaffer, N., Loth, F., 2013. Variability of computational fluid dynamics solutions for pressure and flow in a giant aneurysm: The ASME 2012 summer bioengineering conference CFD challenge. J. Biomech. Eng. 135, 021016. https://doi.org/10.1115/1.4023382.

Voss, S., Arens, C., Janiga, G., 2018. Assessing transitional air flow during human exhalation from large eddy simulations based on spectral entropy. Flow, Turbul. Combust., 1–12 https://doi.org/10.1007/s10494-018-9894-6.